V European Conference on Computational Fluid Dynamics
ECCOMAS CFD 2010
J. C. F. Pereira and A. Sequeira (Eds)
Lisbon, Portugal,14-17 June 2010

A C/DG-FEM SOLUTION OF AN IMPROVED BOUSSINESQ SYSTEM FOR SURFACE WATER WAVES

N. D. Lopes[1,2,3,†], P. J. S. Pereira[1,4] and L. Trabucho[2,3]

[1]Dep. Matemática, ISEL, R. Conselheiro Emidio Navarro, 1, 1959-007 Lisboa, Portugal
[2]Dep. Matemática, FCT, Universidade Nova de Lisboa, 2829-516 Caparica, Portugal
[3]CMAF, Av. Prof. Gama Pinto, 2, 1649-003 Lisboa, Portugal
[4]CEFITEC, FCT, Universidade Nova de Lisboa, 2829-516 Caparica, Portugal
[†] e-mail: ndl@ptmat.fc.ul.pt

Key words: Boussinesq equations; surface water waves; continuous/discontinuous finite element methods

Abstract. *An improved class of Boussinesq systems of fourth order, using wave elevation and velocity potential formulation is derived. Dissipative effects and wave generation due to time dependent varying sea bed are included. Thus, high-order source functions are considered. With the inclusion of an extra $O(h_0\mu^6)$ term in the velocity potential expansion, with h_0 the constant part of the depth $h = h_0 + h_1(x, y, t)$, we are able to reduce the system order maintaining some dispersive characteristics of the higher-order ones. We introduce a nonlocal continuous/discontinuous Galerkin finite element method (C/DG-FEM) with inner penalty terms to approximate the solutions of the fourth-order models. Improved stability is achieved. To demonstrate the applicability of the model, several test cases are considered.*

1 INTRODUCTION

We implement a solver for some of the Boussinesq type systems to model the evolution of surface water waves in a variable depth seabed. This type of models is used, for instance, in harbour simulation, tsunami generation and propagation as well as in coastal dynamics.

There are several **B**oussinesq models and some of the most widely used are those based on the wave **E**levation and horizontal **V**elocities formulation (BEV) (see, e.g., [1, 2]).

In the next section, the governing equations for surface water waves are presented. From these equations different types of models can be derived. We consider only the wave **E**levation and velocity **P**otential (BEP) formulation (see, e.g., [3]). Thus, the number of system equations is reduced when compared to the BEV models.

In the subsequent sections, we derive a class of improved fourth and sixth-order models, which are derived in order to maintain some of the dispersive characteristics of the higher order ones. These models are complemented with the inclusion of effects like dissipation and wave generation by moving an impermeable bottom. In our approach, instead of the assumption of a slowly varying bottom (cf., e.g., [4]), we make a decomposition of the bottom in the form $h(x, y, t) = h_0 + h_1(x, y, t)$.

An important characteristic of the derived models, including dissipative effects, is presented in the fourth section, namely, the dispersion relation.

In the fifth section, we describe several types of wave generation, absorption and reflection mechanisms. Total reflective walls are modelled by homogeneous Neumann conditions.

The second part of the work is presented in the following sections. The sixth section is dedicated to the numerical methods used in the discretization of the variational formulation of the improved fourth-order model. We propose a continuous/discontinuous finite element method (C/DG-FEM) with inner penalty terms to approximate the solutions of the problem. Note that this type of methods uses the same number of degrees of freedom as the standard continuous finite element methods. This scheme has nonlocal characteristics since we encounter terms on interior boundaries contributing to the two elements adjacent to the respective interfaces. In consequence, it requires an additional loop over interior boundaries (cf. [5]). This feature is provided by the open source libraries from the `FEniCS` project [6] and described in the work by Olgaard et al. [7]. The discretization of the spatial variables is accomplished with low order Lagrange finite elements whereas the time integration is implemented using Runge-Kutta and Predictor-Corrector algorithms. Thus, the presented scheme stands as an alternative to the discontinuous local schemes proposed for other Boussinesq models (cf., e.g., [8, 9]). Concerning the usage of FEM methods in this type of problems we also refer the works of P. Avillez-Valente and F.J. Seabra Santos [10] as well as Codina et al. [11]. In the first work a Petrov-Galerkin scheme is presented for an high-order BEV model. In the second paper a subgrid scale stabilized FEM is developed.

We have been developing `DOLFWAVE` [12], i.e., a `FEniCS` based application for BEP models which incorporates the numerical implementation of the presented fourth-order model as well as some other second-order ones.

In the seventh section we validate the model and numerical scheme with test cases. Good agreement between the solutions of several models and improved stability is achieved.

2 MODEL DERIVATION

As usual we consider the following set of equations for the irrotational flow of an incompressible and inviscid fluid:

$$\begin{cases} \dfrac{\partial \vec{u}}{\partial t} + (\vec{u}\cdot\nabla_{xyz})\vec{u} = -\nabla_{xyz}\left(\dfrac{P}{\rho} + g\,z\right), \\ \nabla_{xyz}\times\vec{u} = \vec{0}, \\ \nabla_{xyz}\cdot\vec{u} = 0, \end{cases} \tag{1}$$

where $\vec{u}$ is the velocity vector field of the fluid, P the pressure, g the gravitational acceleration, ρ the mass per unit volume, t the time and the differential operator $\nabla_{xyz} = \left(\frac{\partial}{\partial x}, \frac{\partial}{\partial y}, \frac{\partial}{\partial z}\right)$. A Cartesian coordinate system is adopted with the horizontal x and y-axes on the still water plane and the z-axis pointing vertically upwards (see Fig. 1). The fluid domain is bounded by the bottom seabed at $z = -h(x,y,t)$ and the free water surface at $z = \eta(x,y,t)$. In Fig. 1, L, A and H are the characteristic wave length, wave amplitude

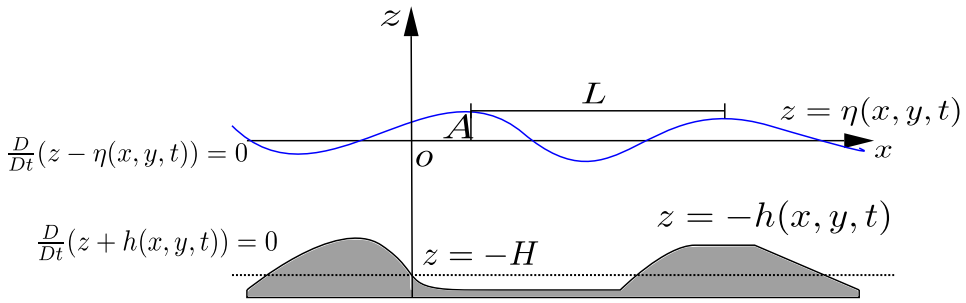

Figure 1: Cross-section of the water wave domain.

and depth, respectively. Note that the material time derivative is denoted by $\frac{D}{Dt}$.

From the irrotational assumption (see $(1)_2$), one can introduce a velocity potential function, $\phi(x,y,z,t)$, to obtain Bernoulli's equation:

$$\frac{\partial \phi}{\partial t} + \frac{1}{2}\nabla_{xyz}\phi\cdot\nabla_{xyz}\phi + \frac{P}{\rho} + g\,z = f(t), \tag{2}$$

where $f(t)$ stands for an arbitrary function of integration. Note that one can remove $f(t)$ from equation (2) if ϕ is redefined by $\phi + \int f(t)\,\mathrm{d}t$. From the incompressibility condition

(see $(1)_3$) the velocity potential satisfies Laplace's equation:

$$\nabla^2\phi + \frac{\partial^2\phi}{\partial z^2} = 0, \tag{3}$$

where ∇ is the horizontal gradient operator given by $\nabla = \left(\frac{\partial}{\partial x}, \frac{\partial}{\partial y}\right)$. To close this problem, the following boundary conditions must be satisfied:

i) the kinematic boundary condition for the free water surface:

$$\frac{\partial\phi}{\partial z} = \frac{\partial\eta}{\partial t} + \nabla\phi\cdot\nabla\eta + D_1(\eta), \quad z = \eta; \tag{4}$$

ii) the kinematic boundary condition for the impermeable sea bottom:

$$\frac{\partial\phi}{\partial z} + (\nabla\phi\cdot\nabla h) = -\frac{\partial h}{\partial t}, \quad z = -h; \tag{5}$$

iii) the dynamic boundary condition for the free water surface:

$$\frac{\partial\phi}{\partial t} + g\eta + \frac{1}{2}\left(|\nabla\phi|^2 + \left(\frac{\partial\phi}{\partial z}\right)^2\right) + D_2(\phi) = 0, \quad z = \eta, \tag{6}$$

where $D_i(\phi)(i = 1, 2)$ is a dissipative term (see, e.g., the work by Duthyk and Dias [13, 14]). We assume that these dissipative terms are of the following form:

$$D_1(\phi) = -\nu_1\nabla^2\eta, \quad D_2(\phi) = \nu_2\frac{\partial^2\phi}{\partial z^2}, \tag{7}$$

with $\nu_i = \dfrac{\bar{\mu_i}}{\rho}$ and $\bar{\mu_i}$ an eddy-viscosity coefficient $(i = 1, 2)$. Note that a nondissipative model means that there is no energy loss. This is not acceptable from a physical point of view, since any real flow is accompanied by energy dissipation.

Note that using Laplace's equation it is possible to rewrite $(7)_2$ as $D_2(\phi) = -\nu_2\nabla^2\phi$. Throughout the literature, analogous terms (sponge layers) were added to the kinematic and dynamic conditions to absorb the wave energy near the boundaries.

A more detailed description of the above equations is found in G. B. Whitham's reference book on waves [15], or in the more recent book by R. S. Johnson [16].

To transform equations (3)-(7) in a dimensionless form, the following scales are introduced:

$$(x', y') = \frac{1}{L}(x, y), \quad z' = \frac{z}{H}, \quad t' = \frac{t\sqrt{gH}}{L}, \quad \eta' = \frac{\eta}{A}, \quad \phi' = \frac{H\phi}{AL\sqrt{gH}}, \quad h' = \frac{h}{H}, \tag{8}$$

together with the small parameters

$$\mu = \frac{H}{L}, \quad \varepsilon = \frac{A}{H}. \tag{9}$$

In the last equation, μ is usually called the long wave parameter and ε the small amplitude wave parameter. Note that ε is related with the nonlinear terms and μ with the dispersive terms. For simplicity, in what follows, we drop the prime notation.

The Boussinesq approach consists in reducing a 3**D** problem to a 2**D** one. This may be accomplished by expanding the velocity potential in a Taylor power series in terms of z. Using Laplace's equation, in a dimensionless form, one can obtain the following expression for the velocity potential:

$$\phi(x,y,z,t) = \sum_{n=0}^{+\infty} \left((-1)^n \frac{z^{2n}}{(2n)!} \mu^{2n} \nabla^{2n} \phi_0(x,y,t) + (-1)^n \frac{z^{2n+1}}{(2n+1)!} \mu^{2n} \nabla^{2n} \phi_1(x,y,t) \right), \tag{10}$$

with

$$\phi_0 = \phi \mid_{z=0}, \quad \phi_1 = \left(\frac{\partial \phi}{\partial z} \right) \mid_{z=0}. \tag{11}$$

From asymptotic expansions, successive approximation techniques and using the kinematic boundary condition for the sea bottom, it is possible to write ϕ_1 in terms of ϕ_0 (cf., e.g., [3, 17]). In this work, without loss of generality, we assume that the dispersive and nonlinear terms are related by the following equation:

$$\frac{\varepsilon}{\mu^2} = O(1). \tag{12}$$

Note that the Ursell number is defined by $U_r = \dfrac{\varepsilon}{\mu^2}$. The dimensionless eddy-viscosity parameters $\hat{\nu}_1$ and $\hat{\nu}_2$ are given by:

$$\hat{\nu}_i = \nu_i \frac{L}{\sqrt{gH} H^2} \mu^2 \quad (i = 1, 2). \tag{13}$$

We assume that $\hat{\nu}_i \, (i = 1, 2)$ is of order $O(\mu^2)$.

In our approach we decompose the dimensionless depth h in the form:

$$h(x,y,t) = h_0 + h_1(x,y,t) \tag{14}$$

with h_0 a reference constant and h_1 an $O(\mu^{1/4})$ perturbation of the dimensionless sea bottom. In this framework ϕ_1 is rewritten as follows:

$$\begin{aligned} \phi_1 = & -\mu^2 \nabla \cdot (h \nabla \phi_0) + \frac{\mu^4}{6} \nabla \cdot \left(h^3 \nabla^3 \phi_0 \right) - \frac{\mu^4}{2} \nabla \cdot \left(h^2 \nabla^2 \cdot (h \nabla \phi_0) \right) - \\ & - \mu^6 h_0^5 \frac{2}{15} \nabla^6 \phi_0 - \frac{\mu^2}{\varepsilon} \frac{\partial h}{\partial t} - \frac{\mu^2}{\varepsilon} \frac{\mu^2}{2} \nabla \cdot \left(h^2 \nabla \frac{\partial h}{\partial t} \right) - \frac{\mu^2}{\varepsilon} \frac{5 h_0^4 \mu^4}{24} \nabla^4 \frac{\partial h}{\partial t} + O(\mu^7). \end{aligned} \tag{15}$$

Note that the dispersive terms of order $O(\mu^6)$ that are only dependent on the constant depth are kept, i.e., the model equations retain the terms up to the order $O(\mu^2, h_0\mu^4, \varepsilon, h_0\mu^2\varepsilon)$.

Our goal is to derive a complete fourth-order model with an extra sixth-order term. This term is only associated with the constant depth factor. In this framework, some properties of the higher-order models are maintained. The resulting model is given by:

$$\begin{bmatrix} \mathcal{T}_h^1(\eta) \\ \mathcal{T}_h^2(\phi_0) \end{bmatrix} + \begin{bmatrix} \mathcal{L}_h^1(\eta) \\ \mathcal{L}_h^2(\phi_0) \end{bmatrix} + \begin{bmatrix} \mathcal{L}_h^3(\phi_0) \\ \mathcal{L}_h^4(\eta) \end{bmatrix} + \begin{bmatrix} \mathcal{N}_h^1(\eta, \phi_0) \\ \mathcal{N}_h^2(\eta, \phi_0) \end{bmatrix} = \begin{bmatrix} \mathcal{S}_1(h) \\ \mathcal{S}_2(h) \end{bmatrix}, \tag{16}$$

with

$$\begin{cases} \mathcal{T}_h^1(\eta) = \dfrac{\partial \eta}{\partial t}, \quad \mathcal{T}_h^2(\phi_0) = \dfrac{\partial \phi_0}{\partial t}, \\ \mathcal{L}_h^1(\eta) = -\hat{\nu}_1 \nabla^2 \eta, \quad \mathcal{L}_h^2(\phi_0) = -\hat{\nu}_2 \nabla^2(\phi_0) + \mu^2 h_0 \nabla^2 \phi_0 \dfrac{\partial h}{\partial t}, \\ \mathcal{L}_h^3(\phi_0) = \nabla \cdot (h \nabla \phi_0) - \dfrac{\mu^2}{6} \nabla \cdot \left(h^3 \nabla^3 \phi_0\right) + \dfrac{\mu^2}{2} \nabla \cdot \left(h^2 \nabla^2 \cdot (h \nabla \phi_0)\right) + \mu^4 h_0^5 \dfrac{2}{15} \nabla^6 \phi_0, \\ \mathcal{L}_h^4(\eta) = \eta - \mu^2 \eta \dfrac{\partial^2 h}{\partial t^2}, \\ \mathcal{N}_h^1(\eta, \phi_0) = \varepsilon \nabla \cdot (\eta \nabla \phi_0), \quad \mathcal{N}_h^2(\eta, \phi_0) = \dfrac{\varepsilon}{2} |\nabla \phi_0|^2 + \dfrac{1}{2} \varepsilon \mu^2 h_0^2 \left(\nabla^2 \phi_0\right)^2 - \varepsilon \eta \mu^2 h_0 \nabla^2 \dfrac{\partial \phi_0}{\partial t}, \\ \mathcal{S}_1(h) = -\dfrac{1}{\varepsilon} \dfrac{\partial h}{\partial t} - \dfrac{1}{\varepsilon} \dfrac{\mu^2}{2} \nabla \cdot \left(h^2 \nabla \dfrac{\partial h}{\partial t}\right) - \dfrac{1}{\varepsilon} \dfrac{5 h_0^4 \mu^4}{24} \nabla^4 \dfrac{\partial h}{\partial t}, \quad \mathcal{S}_2(h) = -\dfrac{1}{2} \dfrac{\mu^2}{\varepsilon} \left(\dfrac{\partial h}{\partial t}\right)^2. \end{cases} \tag{17}$$

Note that $\dfrac{\partial h}{\partial t}$ is assumed to be of order $O(\mu^2, \varepsilon)$ (cf. [18]). Since the Boussinesq models are, in general, composed of a very high number of terms, we express all the systems in the above matrix notation.

Taking into account the variable transformation:

$$\phi_0 = \Phi - \frac{2}{15} \mu^4 h_0^4 \nabla^4 \phi_0, \tag{18}$$

we deduce the improved 4^{th}-order model given by (16) and (17), replacing in (17) ϕ_0 by Φ as well as $\mathcal{T}_h^2$ and $\mathcal{L}_h^3$ by the following expressions:

$$\begin{cases} \mathcal{T}_h^2(\Phi) = \dfrac{\partial \Phi}{\partial t} - \dfrac{2}{15} \mu^4 h_0^4 \nabla^4 \dfrac{\partial \Phi}{\partial t}, \\ \mathcal{L}_h^3(\Phi) = \nabla \cdot (h \nabla \Phi) - \dfrac{\mu^2}{6} \nabla \cdot \left(h^3 \nabla^3 \Phi\right) + \dfrac{\mu^2}{2} \nabla \cdot \left(h^2 \nabla^2 \cdot (h \nabla \Phi)\right). \end{cases} \tag{19}$$

3 MODEL IMPROVEMENTS

As we will see in the next section, in order to improve the linear dispersion properties, it is useful to replace ϕ_0 by an auxiliary function denoted by Φ_α. In our work Φ_α is given by

$$\Phi_\alpha = \phi_\alpha + B \mu^4 h_0^4 \nabla^4 \phi_\alpha, \tag{20}$$

with $\phi_\alpha = \phi(x, y, -\alpha h, t)$ the flow potential evaluated at an arbitrary level $z = -\alpha h, \alpha \in [0, 1]$ (see, e.g., [19, 20]) and B a real constant depending on α.

Using successive approximations (or an asymptotic expansion in ϕ_0) we are able to express ϕ_0 in terms of ϕ_α:

$$\begin{aligned}\phi_0 = \phi_\alpha + \mu^2 \left(-\alpha h \nabla \cdot (h \nabla \phi_\alpha) + \frac{(\alpha h)^2}{2} \nabla^2 \phi_\alpha\right) + \\ + \mu^4 \left(\frac{5}{24}\alpha^4 - \frac{5}{6}\alpha^3 + \alpha^2 - \frac{\alpha}{3}\right) h_0^4 \nabla^4 \phi_\alpha - (\alpha h)\frac{\mu^2}{\varepsilon}\frac{\partial h}{\partial t} + \mu^2 \frac{\mu^2}{\varepsilon}\left(-\frac{\alpha^3}{3} + \alpha^2 - \frac{\alpha}{2}\right) h_0^3 \nabla^2 \frac{\partial h}{\partial t}.\end{aligned} \tag{21}$$

Now we can use (20) and (21) to replace ϕ_0 by Φ_α in (16) and (17).

As a consequence we are able to propose a class of improved models described as follows:

$$\begin{cases} \mathcal{T}_h^1(\eta) = \dfrac{\partial \eta}{\partial t}, \\ \mathcal{T}_h^2(\Phi_\alpha) = \dfrac{\partial \Phi_\alpha}{\partial t} - \mu^2 \alpha \dfrac{\partial}{\partial t}\left(h \nabla \cdot (h \nabla \Phi_\alpha)\right) + \mu^2 \dfrac{\alpha^2}{2}\dfrac{\partial}{\partial t}\left(h^2 \nabla^2 \Phi_\alpha\right) + \mu^4 B_0 h_0^4 \dfrac{\partial}{\partial t}\nabla^4 \Phi_\alpha, \\ \mathcal{L}_h^1(\eta) = -\hat{\nu}_1 \nabla^2 \eta - \alpha \mu^2 h_0 \nabla \cdot \left(\eta \nabla \dfrac{\partial h}{\partial t}\right), \\ \mathcal{L}_h^2(\Phi_\alpha) = -\alpha h_0 \mu^2 \nabla \Phi_\alpha \nabla \dfrac{\partial h}{\partial t} - \hat{\nu}_2 \nabla^2(\Phi_\alpha) - \hat{\nu}_2 B_1 \mu^2 h_0^2 \nabla^4 \Phi_\alpha + \mu^2 h_0 \nabla^2 \Phi_\alpha \dfrac{\partial h}{\partial t}, \\ \mathcal{L}_h^3(\Phi_\alpha) = \nabla \cdot (h \nabla \Phi_\alpha) - \dfrac{\mu^2}{6}\nabla \cdot \left(h^3 \nabla^3 \Phi_\alpha\right) + \dfrac{\mu^2}{2}\nabla \cdot \left(h^2 \nabla^2 \cdot (h \nabla \Phi_\alpha)\right) + \mu^4 h_0^5 B_2 \nabla^6 \Phi_\alpha, \\ \quad -\alpha \mu^2 \nabla \cdot \left(h \nabla \left(h \nabla \cdot (h \nabla \Phi_\alpha)\right)\right) + \dfrac{\alpha^2}{2}\mu^2 \nabla \cdot \left(h \nabla \left(h^2 \nabla^2 \Phi_\alpha\right)\right), \\ \mathcal{L}_h^4(\eta) = \eta - \mu^2 \eta \dfrac{\partial^2 h}{\partial t^2}, \\ \mathcal{N}_h^1(\eta, \Phi_\alpha) = \varepsilon \nabla \cdot (\eta \nabla \Phi_\alpha) + \mu^2 \varepsilon B_1 h_0^2 \nabla \cdot (\eta \nabla^3 \Phi_\alpha), \\ \mathcal{N}_h^2(\eta, \Phi_\alpha) = \dfrac{\varepsilon}{2}\left|\nabla \Phi_\alpha\right|^2 + \dfrac{1}{2}\varepsilon \mu^2 h_0^2 \left(\nabla^2 \Phi_\alpha\right)^2 + \mu^2 h_0^2 \varepsilon \nabla \Phi_\alpha \nabla^3 \Phi_\alpha + \varepsilon \eta \mu^2 h_0 \nabla^2 \eta, \\ \mathcal{S}_1(h) = -\dfrac{1}{\varepsilon}\dfrac{\partial h}{\partial t} - \dfrac{1}{\varepsilon}\dfrac{\mu^2}{2}\nabla \cdot \left(h^2 \nabla \dfrac{\partial h}{\partial t}\right) + \mu^2 \dfrac{\mu^2}{\varepsilon} B_3 h_0^4 \nabla^4 \dfrac{\partial h}{\partial t} + \alpha \dfrac{\mu^2}{\varepsilon}\nabla \cdot \left(h \nabla (h \dfrac{\partial h}{\partial t})\right), \\ \mathcal{S}_2(h) = -\dfrac{1}{2}\dfrac{\mu^2}{\varepsilon}\left(\dfrac{\partial h}{\partial t}\right)^2 + \alpha \dfrac{\mu^2}{\varepsilon}\dfrac{\partial}{\partial t}\left(h \dfrac{\partial h}{\partial t}\right) - \mu^2 \dfrac{\mu^2}{\varepsilon} B_4 h_0^3 \nabla^2 \dfrac{\partial^2 h}{\partial t^2} - \alpha h_0 \hat{\nu}_2 \dfrac{\mu^2}{\varepsilon}\nabla^2 \left(\dfrac{\partial h}{\partial t}\right), \end{cases} \tag{22}$$

where B, $B_0, \cdots, B_4$ are α dependent and $\mathcal{R}^\alpha_{(\cdot)}$ is defined by:

$$\mathcal{R}^\alpha_{p \pm q} = (\alpha - p + q)(\alpha - p - q), \quad \mathcal{R}^\alpha_p = (\alpha - p), \quad p, q \in \mathbb{R}. \tag{23}$$

We obtain the following sets of coefficients for the two models. For the first case (6o-A) we have a 6^{th}-order model with $\alpha \neq 0$ and

$$B_0 = \frac{5}{24}\alpha \mathcal{R}_2^\alpha \mathcal{R}^\alpha_{1 \pm \sqrt{5}/5}, \quad B_2 = \frac{5}{24}\left(\mathcal{R}^\alpha_{1 \pm \sqrt{5}/5}\right)^2, \quad B = 0. \tag{24}$$

The second case (4o-A) is the 4^{th}-order model with $\alpha \neq 0$ and

$$B_0 = -\frac{1}{6}\mathcal{R}^{\alpha}_{1\pm\sqrt{5}/5}, \quad B_2 = 0, \quad B = \frac{5}{24}\left(\mathcal{R}^{\alpha}_{1\pm\sqrt{5}/5}\right)^2. \tag{25}$$

For the two cases we have:

$$B_1 = \frac{1}{2}\alpha\mathcal{R}^{\alpha}_{2}, \quad B_3 = \frac{1}{3}\alpha\mathcal{R}^{\alpha}_{3/2\pm i1/2} - \frac{5}{24}, \quad B_4 = -\frac{1}{3}\alpha\mathcal{R}^{\alpha}_{3/2\pm\sqrt{3}/2}. \tag{26}$$

To finish this section, we just recall that if $\alpha = 0$ we recover the models given in section 2. Namely, if $B_0 = 0$, $B_2 = 2/15$ and $B = 0$ the sixth-order system presented in (16) and (17) arises and if $B_0 = -2/15$, $B_2 = 0$ and $B = 2/15$ we recover the fourth-order system presented in (16) and (17)–(19). On the other hand if we take $\alpha = 1 - \sqrt{5}/5$, the model given by (16), (22)–(24) could be reduced to a 4th-order system since in this case $B_2 = 0$. We show in the next section that the last case has the same dispersion relation as the model proposed in [4].

We stress that if we do not consider in (15) the extra $O(h_0\mu^6)$ terms then we obtain the generalization of the model proposed by Chen and Liu [3] to a time dependent sea bed. In the following section, we illustrate the improvement over the referred model.

4 DISPERSION RELATION

In this section, we present the dispersion relation for the linearized model with a constant depth. We use the standard procedure available throughout the literature (cf, e.g., [21]). For simplicity only the 2**D** case is taken into account and a constant depth ($h = H$) is assumed. The dimensional variables are used throughout this section.

We start by introducing the linearized equations for the full potential flow with dissipative effects:

$$\begin{cases} \dfrac{\partial^2\phi}{\partial z^2} + \nabla^2\phi = 0, \quad (x,z) \in \mathbb{R}\times[-h,0] \\ \dfrac{\partial\eta}{\partial t} - \dfrac{\partial\phi}{\partial z} - \nu_1\nabla^2\eta = 0, \quad z = 0 \\ \dfrac{\partial\phi}{\partial t} + g\eta - \nu_2\nabla^2\phi = 0, \quad z = 0 \\ \dfrac{\partial\phi}{\partial z} = 0, \quad z = -h. \end{cases} \tag{27}$$

This problem admits solutions defined by:

$$\eta(x,t) = a\,\exp(i(kx-\omega t)), \quad \phi(x,z,t) = b^*(z)\exp(i(kx-wt)), \tag{28}$$

as long as the following dispersion relations are satisfied:

$$\omega_1^2 = -\frac{1}{4}(\nu_1-\nu_2)^2k^4 + gHk^2\frac{\tanh(kH)}{kH}, \tag{29}$$

$$\omega_2 = -\frac{k^2}{2}(\nu_1 + \nu_2). \tag{30}$$

We consider that the angular frequency is defined by $\omega = \omega_1 + i\omega_2$ with $\omega_i \in \mathbb{R}\,(i = 1, 2)$, where a is the wave amplitude, $b^*(z)$ is a function related with the potential magnitude and $k = \frac{2\pi}{L}$ is the wave number. If one has $\nu_1 = \nu_2$ then the dissipative terms do not contribute to the real part of the angular frequency.

On the other hand, the linearization of the system described by (16), (22), (24)–(26) with a constant depth ($h = H$), could be written in the generic form:

$$\begin{cases} \dfrac{\partial \eta}{\partial t} + H\nabla^2\Phi_\alpha + B_5 H^3\nabla^4\Phi_\alpha + B_2 H^5\nabla^6\Phi_\alpha - \nu_1\nabla^2\eta = 0, \\ \dfrac{\partial \Phi_\alpha}{\partial t} + B_1 H^2\nabla^2\dfrac{\partial \Phi_\alpha}{\partial t} + B_0 H^4\nabla^4\dfrac{\partial \Phi_\alpha}{\partial t} + g\eta - \nu_2\nabla^2\Phi_\alpha - \\ -\nu_2 B_1 H^2\nabla^4\Phi_\alpha = 0, \end{cases} \tag{31}$$

with $B_5 = \frac{1}{2}\mathcal{R}^{\alpha}_{1\pm\sqrt{3}/3}$.

System (31) admits solutions of the form:

$$\eta(x,t) = a\exp(i(kx - \omega t)), \quad \phi(x,t) = -ib\exp(i(kx - wt)), \tag{32}$$

as long as the associated dispersion relations are satisfied:

$$\omega_1^2 = -\frac{1}{4}\left(\frac{T_4}{T_2}\nu_1 + \frac{T_3}{T_2}\nu_2\right)^2 k^4 + \frac{T_3}{T_2}\nu_1\nu_2 k^4 + gHk^2\frac{T_1}{T_2}, \tag{33}$$

$$\omega_2 = -\frac{k^2}{2}\left(\frac{T_4}{T_2}\nu_1 + \nu_2\frac{T_3}{T_2}\right), \tag{34}$$

with b the potential magnitude and $T_i\,(i = 1, \cdots, 4)$ given by:

$$\begin{array}{ll} T_1 = 1 - B_5(Hk)^2 + B_2(Hk)^4, & T_2 = 1 - B_1(Hk)^2 + B_0(Hk)^4, \\ T_3 = 1 - B_1(Hk)^2, & T_4 = 1 - B_2(Hk)^2 + B_0(Hk)^4. \end{array} \tag{35}$$

Now we discuss the choice for the value of α. The main idea is to optimize the coefficients $T_i\,(i = 1, \cdots, 4)$ in (33) and (34) in order to reproduce (29) and (30). Note that the effects of the dissipative terms in the presented Boussinesq systems are not taken into account, i.e., $\nu_1 = \nu_2 = 0$.

It is usual to compare the dispersion relations of the derived models with Padé's expansions of the one given by the full linear theory (see, e.g., [20, 22]). The normalized square of the phase velocity $\bar{C}_p^2$ is defined by:

$$\bar{C}_p^2 = \frac{\omega^2}{gHk^2} = \frac{\tanh(kH)}{kH}. \tag{36}$$

The Padé's expansions of order $[2,2]$ and $[2,4]$ of $\bar{C}_p^2$ are given by:

$$i) \quad \frac{1+(kH)^2/15}{1+2(kH)^2/5}, \qquad ii) \quad \frac{1+2(kH)^2/21}{1+3(kH)^2/7+(kH)^4/105}, \tag{37}$$

respectively. We can choose α in order that $\left(\frac{T_1}{T_2}\right)$ reproduces the expansions presented in (37). Namely, $\alpha = 1-\sqrt{5}/5$ and $\alpha = 1-\sqrt{7}/7$ reproduce $(37)_{i)}$ and $(37)_{ii)}$, respectively. Note that for $\alpha = 1-\sqrt{5}/5$ both cases 6o-A and 4o-A are the same. For this case we obtain the dispersion relations presented, for instance, in the second-order model of Zhao et al. [4]. In Fig. 2 we present $\bar{C}_p^2$, relative to our model, together with that one of the Chen and Liu's model as a function of kH. We stress that it is possible to

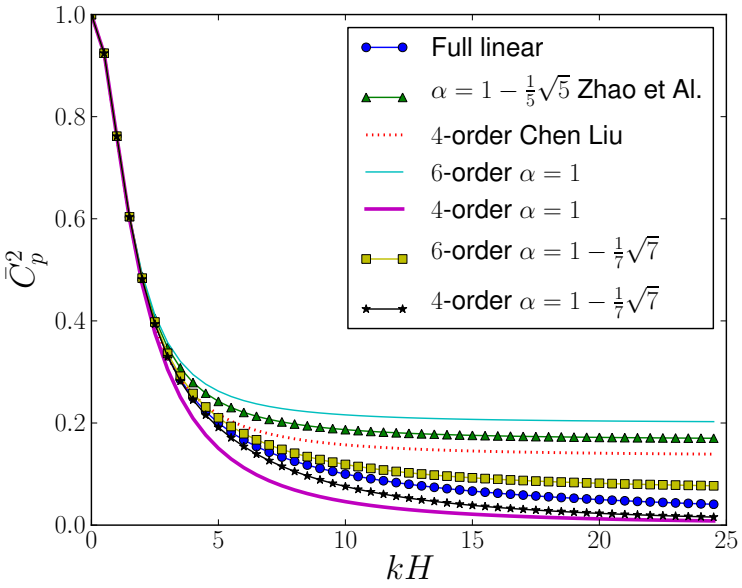

Figure 2: The normalized square of the phase velocity as a function of kH. Chen and Liu dispersion relations are also presented.

improve the dispersion relation approximation with another value of α, if we consider as the optimization criterion, for instance, the relative least-square error between the dispersion relations. As an example, we refer the following errors obtained for a fixed interval $kH \in [0,20]$: for $\alpha = 1-\sqrt{5}/5$ an $\approx 8.6\%$ error is obtained; for $\alpha = 1$ the error of the fourth-order model is improved to $\approx 2.39\%$ and if $\alpha = 1-\sqrt{7}/7$ we obtain $\approx 0.49\%$ and $\approx 0.55\%$ errors relative to the sixth and fourth-order models, respectively. We note that the error produced by the [4,4] Padé's approximation is $\approx 0.29\%$. Nevertheless, if one chooses $\alpha = 0.583948$ we can improve the dispersion relation obtaining an 0.08% error for the 4o-A model.

5 BOUNDARY CONDITIONS

In this section some of the physical mechanisms to induce, absorb or reflect surface water waves are presented. We note that the moving bottom approach is useful for wave generation due to seismic activities. However, some physical applications are associated with other wave generation mechanisms.

Sometimes called passive generation, the simplest way of inducing a wave into a certain domain is to consider an appropriate initial condition. This is the case presented in the first numerical test (see subsection 7.1).

For time-dependent wave generation, it is possible to consider waves induced by a boundary condition. This requires that the wave surface elevation and the velocity potential must satisfy appropriated boundary conditions, e.g., Dirichlet or Neumann conditions. We do not use this method in this work. Nevertheless, this method is implemented in some of our examples in the `DOLFWAVE` library (see [12]).

Besides the incident wave boundaries where the wave profiles are given, one must close the system with appropriate boundary conditions. Let us denote Γ as the boundary of Ω and Γ_r as the subset of Γ where reflective boundaries are considered.

We consider two more types of boundaries:

i) full reflective boundaries;

ii) partial reflective or absorbing boundaries.

The first case is modelled by the following equations:

$$\begin{cases} \nabla^{2n-1}\Phi_\alpha \cdot \mathbf{n} = 0, \forall n = 1, 2 \\ \nabla\eta \cdot \mathbf{n} = 0, \end{cases} \quad \forall (x, y) \in \Gamma_r \tag{38}$$

where $\mathbf{n}$ is the outward unit vector normal to the computational domain Ω (see [9]).

Coupling the reflective case and an extra artificial layer, often called sponge or damping layer, we can simulate partial reflective or full absorbing boundaries. In this way, the reflected energy can be controlled. Moreover, one can prevent unwanted wave reflections and avoid complex wave interactions. It is also possible to simulate effects like energy dissipation by wave breaking.

6 NUMERICAL METHOD

In this section, we introduce a continuous/discontinuous finite element formulation for the fourth-order Boussinesq model described by equations (16), (22) and (25)–(26). Our numerical scheme arises from the concepts introduced by Engel et al. [5] for the fourth-order elliptic problems in structural and continuum mechanics. In what follows, we just consider the Neumann boundary conditions, since the Dirichlet boundary conditions are applied in the classical way.

In order to implement the interior penalty continuous/discontinuous finite element method, let us define the finite-dimensional trial solution and weighting function spaces as follows:

$$\mathscr{A}^{\boldsymbol{h}} = \mathscr{B}^{\boldsymbol{h}} = \mathscr{V}^{\boldsymbol{h}} = \{\vartheta^{\boldsymbol{h}} \in H^1(\Omega) \,|\, \vartheta^{\boldsymbol{h}}|_{\Omega_e} \in P_2(\Omega_e)\, \forall \Omega_e \in \mathscr{P}(\Omega)\}, \tag{39}$$

where $\mathscr{P}(\Omega) = \{\Omega_e\}_{e=1}^{N_e}$ is a regular and triangular finite element partition of the polygonal domain Ω into N_e elements Ω_e. $P_2(\Omega_e)$ is the finite-dimensional space of all polynomials of degree less than or equal to 2 defined on Ω_e. The method that we propose for the solution of the problem given by (16), (22) and (25)–(26) can be written as follows: find $\left(\eta^{\boldsymbol{h}}, \Phi_\alpha^{\boldsymbol{h}}\right) \in \mathscr{A}^{\boldsymbol{h}} \times \mathscr{B}^{\boldsymbol{h}}$ such that

$$\begin{cases} a_1\left(\eta_t^{\boldsymbol{h}}, \vartheta_1^{\boldsymbol{h}}\right) = L_1(\eta^{\boldsymbol{h}}, \Phi_\alpha^{\boldsymbol{h}}, \vartheta_1^{\boldsymbol{h}}), \\ a_2\left(\Phi_{\alpha t}^{\boldsymbol{h}}, \vartheta_2^{\boldsymbol{h}}\right) = L_2(\Phi_\alpha^{\boldsymbol{h}}, \eta^{\boldsymbol{h}}, \vartheta_2^{\boldsymbol{h}}), \end{cases} \quad \forall \vartheta_1^{\boldsymbol{h}}, \vartheta_2^{\boldsymbol{h}} \in \mathscr{V}^{\boldsymbol{h}} \tag{40}$$

where a_i and L_i $(i = 1, 2)$ are derived from the variational formulation of the problem and the subscript t denotes the time derivative, for simplicity. In the next equations we use the following notation:

$$(\cdot,\cdot)_{\tilde{\Omega}} = \sum_{e=1}^{N_e} (\cdot,\cdot)_{\Omega_e}, \quad (\cdot,\cdot)_{\tilde{\Gamma}} = \sum_{j=1}^{N_i} (\cdot,\cdot)_{\tilde{\Gamma}_j}, \quad (\cdot,\cdot)_{\Gamma_h} = \sum_{j=1}^{N_h} (\cdot,\cdot)_{\Gamma_j}, \tag{41}$$

with N_i the number of interior boundaries, N_h the number of exterior boundaries and $(\cdot,\cdot)_{\tilde{\Omega}}$ stands for L^2-inner product on element interiors whereas $(\cdot,\cdot)_{\tilde{\Gamma}}$ stands for the L^2-inner product over the interior boundaries. Moreover, the L^2-inner product over the exterior boundaries is denoted by $(\cdot,\cdot)_{\Gamma_h}$.

The jump $[\![\cdot]\!]$ operator is defined as $[\![\mathbf{v}]\!] = \mathbf{v}^+ \cdot \mathbf{n}^+ + \mathbf{v}^- \cdot \mathbf{n}^-$ for a vector-valued function, with $\mathbf{v}^+$ and $\mathbf{v}^-$ the values of $\mathbf{v}$ as seen from Ω_e^+ and Ω_e^-, respectively. Here, $\mathbf{n}^+$ and $\mathbf{n}^-$ denote the outward unit vector normal to the given facet as seen from Ω_e^+ and Ω_e^-, respectively (see Fig. 3). The average operator $\langle\cdot\rangle$ is defined, in a similar way, on the element interfaces by $\langle v \rangle = \frac{1}{2}(v^+ + v^-)$ for a scalar function v. The penalty parameters, on the interior and exterior boundaries, are defined by:

$$\bar{\tau}_i = \frac{\tau_i}{\boldsymbol{h}_e^+}, \quad \bar{\tau}_i^{\boldsymbol{h}} = \frac{\tau_i^{\boldsymbol{h}}}{\boldsymbol{h}_e}, \quad (i = 1, 2), \tag{42}$$

respectively. In (42) $\boldsymbol{h}_e^+$ and $\boldsymbol{h}_e$ are functions of the size of the cells Ω_e^+ and Ω_e, respectively. In the numerical examples we consider $\tau_i = \tau_i^{\boldsymbol{h}} = \tau$ over all the elements $(i = 1, 2)$.

The forms a_i and $L_i\,(i = 1, 2)$ are given by:

$$a_1\left(\eta_t^{\boldsymbol{h}}, \vartheta_1^{\boldsymbol{h}}\right) = \left(\eta_t^{\boldsymbol{h}}, \vartheta_1^{\boldsymbol{h}}\right)_{\tilde{\Omega}} + \bar{\tau}_1 \left(\left[\!\left[\nabla \eta_t^{\boldsymbol{h}}\right]\!\right], \left[\!\left[\nabla \vartheta_1^{\boldsymbol{h}}\right]\!\right]\right)_{\tilde{\Gamma}} + \bar{\tau}_1^{\boldsymbol{h}} \left(\nabla \eta_t^{\boldsymbol{h}} \cdot \mathbf{n}, \nabla \vartheta_1^{\boldsymbol{h}} \cdot \mathbf{n}\right)_{\Gamma_h}, \tag{43}$$

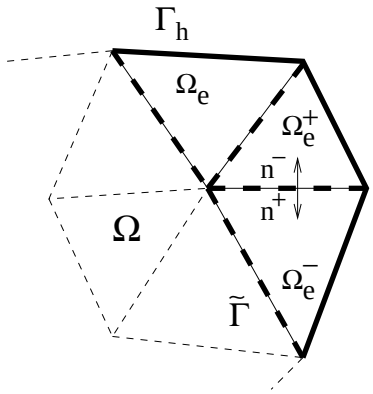

Figure 3: Sketch of a part of a polygonal domain Ω, interior elements Ω_e, boundaries of the interface $\tilde{\Gamma}$ (thicker dashed line) and the domain boundary Γ_h (thicker solid line).

$$
\begin{aligned}
a_2\left(\Phi_{\alpha t}^{\boldsymbol{h}}, \vartheta_2^{\boldsymbol{h}}\right) = & \left(\Phi_{\alpha t}^{\boldsymbol{h}}, \vartheta_2^{\boldsymbol{h}}\right)_{\tilde{\Omega}} + (\alpha-\alpha^2)\left(h\nabla\Phi_{\alpha t}^{\boldsymbol{h}}, \nabla h\,\vartheta_2^{\boldsymbol{h}}\right)_{\tilde{\Omega}} - B_1\left(h\nabla\Phi_{\alpha t}^{\boldsymbol{h}}, h\nabla\vartheta_2^{\boldsymbol{h}}\right)_{\tilde{\Omega}} \\
& + B_0 h_0^4\left(\nabla^2\Phi_{\alpha t}^{\boldsymbol{h}}, \nabla^2\vartheta_2^{\boldsymbol{h}}\right)_{\tilde{\Omega}} - B_0 h_0^4\left(\left\langle\nabla^2\Phi_{\alpha t}^{\boldsymbol{h}}\right\rangle, \left[\!\left[\nabla\vartheta_2^{\boldsymbol{h}}\right]\!\right]\right)_{\tilde{\Gamma}} \\
& - B_0 h_0^4\left(\nabla^2\Phi_{\alpha t}^{\boldsymbol{h}}, \nabla\vartheta_2^{\boldsymbol{h}}\cdot\mathbf{n}\right)_{\Gamma_h} + \bar{\tau}_2\left(\left[\!\left[\nabla\Phi_{\alpha t}^{\boldsymbol{h}}\right]\!\right], \left[\!\left[\nabla\vartheta_2^{\boldsymbol{h}}\right]\!\right]\right)_{\tilde{\Gamma}} + \bar{\tau}_2^{\boldsymbol{h}}\left(\nabla\Phi_{\alpha t}^{\boldsymbol{h}}\cdot\mathbf{n}, \nabla\vartheta_2^{\boldsymbol{h}}\cdot\mathbf{n}\right)_{\Gamma_h}, \quad (44)
\end{aligned}
$$

$$
\begin{aligned}
L_1\left(\eta^{\boldsymbol{h}}, \Phi_\alpha^{\boldsymbol{h}}, \vartheta_1^{\boldsymbol{h}}\right) = & -\nu_1\left(\nabla\eta^{\boldsymbol{h}}, \nabla\vartheta_1^{\boldsymbol{h}}\right)_{\tilde{\Omega}} - \alpha h_0\left(\eta^{\boldsymbol{h}}\nabla h_t, \nabla\vartheta_1^{\boldsymbol{h}}\right)_{\tilde{\Omega}} + \left(h\nabla\Phi_\alpha^{\boldsymbol{h}}, \nabla\vartheta_1^{\boldsymbol{h}}\right)_{\tilde{\Omega}} \\
& + \frac{1}{6}\left(\nabla^2\Phi_\alpha^{\boldsymbol{h}}, \nabla\cdot\left(h^3\nabla\vartheta_1^{\boldsymbol{h}}\right)\right)_{\tilde{\Omega}} - \frac{1}{2}\left(\nabla\cdot\left(h\nabla\Phi_\alpha^{\boldsymbol{h}}\right), \nabla\cdot\left(h^2\nabla\vartheta_1^{\boldsymbol{h}}\right)\right)_{\tilde{\Omega}} \\
& + \alpha\left(h\nabla\cdot\left(h\nabla\Phi_\alpha^{\boldsymbol{h}}\right), \nabla\cdot\left(h\nabla\vartheta_1^{\boldsymbol{h}}\right)\right)_{\tilde{\Omega}} - \frac{\alpha^2}{2}\left(h^2\nabla^2\Phi_\alpha^{\boldsymbol{h}}, \nabla\cdot\left(h\nabla\vartheta_1^{\boldsymbol{h}}\right)\right)_{\tilde{\Omega}} + \left(\eta^{\boldsymbol{h}}\nabla\Phi_\alpha^{\boldsymbol{h}}, \nabla\vartheta_1^{\boldsymbol{h}}\right)_{\tilde{\Omega}} \\
& - B_1 h_0^2\left(\nabla^2\Phi_\alpha^{\boldsymbol{h}}, \nabla\cdot\left(\eta^{\boldsymbol{h}}\nabla\vartheta_1^{\boldsymbol{h}}\right)\right)_{\tilde{\Omega}} + \left(S_1(h), \vartheta_1^{\boldsymbol{h}}\right)_{\tilde{\Omega}} - \frac{1}{6}\left(\left\langle\nabla^2\Phi_\alpha^{\boldsymbol{h}}\right\rangle, \left[\!\left[h^3\nabla\vartheta_1^{\boldsymbol{h}}\right]\!\right]\right)_{\tilde{\Gamma}} \\
& + \frac{\alpha^2}{2}\left(\left\langle h^2\nabla^2\Phi_\alpha^{\boldsymbol{h}}\right\rangle, \left[\!\left[h\nabla\vartheta_1^{\boldsymbol{h}}\right]\!\right]\right)_{\tilde{\Gamma}} + B_1 h_0^2\left(\left\langle\nabla^2\Phi_\alpha^{\boldsymbol{h}}\right\rangle, \left[\!\left[\eta^{\boldsymbol{h}}\nabla\vartheta_1^{\boldsymbol{h}}\right]\!\right]\right)_{\tilde{\Gamma}} \\
& + \left(\frac{1}{2}-\alpha\right)\left(\left\langle\nabla\cdot\left(h\nabla\Phi_\alpha^{\boldsymbol{h}}\right)\right\rangle, \left[\!\left[h^2\nabla\vartheta_1^{\boldsymbol{h}}\right]\!\right]\right)_{\tilde{\Gamma}} + \left(\frac{1}{2}-\alpha\right)\left(\nabla\cdot\left(h\nabla\Phi_\alpha^{\boldsymbol{h}}\right), h^2\nabla\vartheta_1^{\boldsymbol{h}}\cdot\mathbf{n}\right)_{\Gamma_h} \\
& - \frac{1}{6}\left(\nabla^2\Phi_\alpha^{\boldsymbol{h}}, h^3\nabla\vartheta_1^{\boldsymbol{h}}\cdot\mathbf{n}\right)_{\Gamma_h} + \frac{\alpha^2}{2}\left(h^2\nabla^2\Phi_\alpha^{\boldsymbol{h}}, h\nabla\vartheta_1^{\boldsymbol{h}}\cdot\mathbf{n}\right)_{\Gamma_h} + B_1 h_0^2\left(\nabla^2\Phi_\alpha^{\boldsymbol{h}}, \eta^{\boldsymbol{h}}\nabla\vartheta_1^{\boldsymbol{h}}\cdot\mathbf{n}\right)_{\Gamma_h}, \quad (45)
\end{aligned}
$$

$$
\begin{aligned}
L_2\left(\Phi_\alpha^{\boldsymbol{h}},\eta^{\boldsymbol{h}},\vartheta_2^{\boldsymbol{h}}\right) = {} & \alpha h_0\left(\nabla\Phi_\alpha^{\boldsymbol{h}}\nabla h_t,\vartheta_2^{\boldsymbol{h}}\right)_{\tilde\Omega} - \nu_2\left(\nabla\Phi_\alpha^{\boldsymbol{h}},\nabla\vartheta_2^{\boldsymbol{h}}\right)_{\tilde\Omega} + \nu_2 B_1 h_0^2\left(\nabla^2\Phi_\alpha^{\boldsymbol{h}},\nabla^2\vartheta_2^{\boldsymbol{h}}\right)_{\tilde\Omega} \\
& + h_0\left(\nabla\Phi_\alpha^{\boldsymbol{h}},\nabla\left(h_t\vartheta_2^{\boldsymbol{h}}\right)\right)_{\tilde\Omega} - g\left(\eta^{\boldsymbol{h}},\vartheta_2^{\boldsymbol{h}}\right)_{\tilde\Omega} + \left(\eta^{\boldsymbol{h}}h_{tt},\vartheta_2\right)_{\tilde\Omega} - \frac{1}{2}\left(\left|\nabla\Phi_\alpha^{\boldsymbol{h}}\right|^2,\vartheta_2^{\boldsymbol{h}}\right)_{\tilde\Omega} \\
& - \frac{1}{2}h_0^2\left(\left(\nabla^2\Phi_\alpha^{\boldsymbol{h}}\right)^2,\vartheta_2^{\boldsymbol{h}}\right)_{\tilde\Omega} + h_0^2\left(\nabla^2\Phi_\alpha^{\boldsymbol{h}},\nabla\cdot\left(\nabla\Phi_\alpha^{\boldsymbol{h}}\vartheta_2^{\boldsymbol{h}}\right)\right)_{\tilde\Omega} + gh_0\left(\nabla\eta^{\boldsymbol{h}},\nabla\left(\eta^{\boldsymbol{h}}\vartheta_2^{\boldsymbol{h}}\right)\right)_{\tilde\Omega} \\
& - \alpha\left(h\nabla\Phi_\alpha^{\boldsymbol{h}},\nabla\left(h_t\vartheta_2^{\boldsymbol{h}}\right)\right)_{\tilde\Omega} - \alpha\left(h_t\nabla\Phi_\alpha^{\boldsymbol{h}},\nabla\left(h\vartheta_2^{\boldsymbol{h}}\right)\right)_{\tilde\Omega} + \alpha^2\left(\nabla\Phi_\alpha^{\boldsymbol{h}},\nabla\left(hh_t\vartheta_2^{\boldsymbol{h}}\right)\right)_{\tilde\Omega} \\
& + \left(S_2(h),\vartheta_2^{\boldsymbol{h}}\right)_{\tilde\Omega} - \nu_2 B_1 h_0^2\left(\left\langle\nabla^2\Phi_\alpha^{\boldsymbol{h}}\right\rangle,\left[\!\left[\nabla\vartheta_2^{\boldsymbol{h}}\right]\!\right]\right)_{\tilde\Gamma} - \nu_2 B_1 h_0^2\left(\nabla^2\Phi_\alpha^{\boldsymbol{h}},\nabla\vartheta_2^{\boldsymbol{h}}\cdot\mathbf{n}\right)_{\Gamma_h}. \quad (46)
\end{aligned}
$$

Note that the boundary conditions referred in (38) are taken into account. We remark that if the weighting and trial functions are smooth enough, for instance $C^2((0,T);\Omega)$ with T an upper bound for the time variable, then all the penalty terms vanish and we obtain a standard finite element formulation.

The above formulation does not include the (non)symmetrization terms as described in [5] or in the book by Brenner and Scott [23]. Although, we do not obtain significant differences in the solutions, a slight improvement in the stability is achieved if these extra terms are not included. Note that the non penalized formulation is not symmetric.

We use a predictor-corrector scheme with an initialization provided by an explicit Runge-Kutta method for the time integration of (40). We denote the presented numerical model as 4o-M-CDG-P2, standing for mildly nonlinear model discretized by a C/DG-FEM with inner penalty terms using P_2-Lagrange elements.

In the `DOLFWAVE` package, several sets of equations and finite element methods are already implemented. We extend the second-order and $O(\mu^4)$ weakly nonlinear model of Zhao et al. (cf. [4]) in order to consider waves generated by moving bottoms (cf. [17]). This model is spatially discretized using pure continuous Galerkin P_1 or P_2 triangular Lagrange elements, which is denoted by 2o-ZTC-P1 or 2o-ZTC-P2, respectively.

We also consider the weakly nonlinear version, namely, 4o-W-CDG-P2 where only $O(\varepsilon)$ nonlinear terms are taken into account. The same predictor-corrector scheme is considered for all the cases. In the following section, we compare numerical solutions provided by some of the referred models.

7 MODEL VALIDATION

For the model validation, we consider a benchmark available in the literature together with another one. Note that the post-processing of all 3D figures is only made using P_1 elements. No dissipative terms are used in the following tests. In all the cases we assume that the numerical model blows-up if a limit of 5 corrector-steps iterations is exceeded.

7.1 The Gaussian hump in a square basin

For the first test case we simulate the evolution of a Gaussian hump in a square basin. We compare the results with those obtained by Liu and Woo [1], where a weakly nonlinear BEV model is used (cf. [11, 24]).

The computational domain is a 6×6 m^2 square that we discretize using a symmetric uniform mesh with 900 elements and an unstructured triangular mesh with 1998 elements.

Reflective wall boundary conditions are applied which are described by (38). As initial conditions we consider:

$$\begin{cases} \eta(x,y,0) = 0.045\, e^{-2\left((x-3)^2+(y-3)^2\right)} \quad \text{(m)}, \\ \Phi_\alpha(x,y,0) = 0 \quad \text{(m}^2\,\text{s}^{-1}\text{)}. \end{cases} \tag{47}$$

A constant depth $h = 0.45$ m is considered. We also compare the surface elevation given by the proposed fourth-order model with 2o-ZTC-P1 and 2o-ZTC-P2.

In the present simulation the time-steps are given by $\triangle t = 0.0005$ s and $\triangle t = 0.00025$ s for the uniform symmetric and unstructured meshes, respectively. Several values are tested for the penalty coefficients. One can see that higher penalty parameters improve the stability of the scheme. Even though, we do not know the exact solutions of the nonlinear equations, higher values of the penalty parameters produce numerical solutions with a strong dependence on the mesh geometry. Thus, the accuracy of the method is compromised.

In Fig. 4 one can see some surface elevation snapshots at $t_1 = 4$ s and $t_2 = 8$ s provided by 4o-M-CDG-P2 as well as 4o-W-CDG-P2, for the symmetric mesh (left column) and for the unstructured meshes (right column), respectively. As expected, the inclusion of higher order nonlinear terms increases the instability of the model.

In Fig. 5 we show the time history of the surface elevation for two different points of the domain, namely, $P_1 = (3,3)$ m (center of the domain) and $P_2 = (1,1)$ m, using the uniform and unstructured meshes, respectively. We illustrate the blow-up of the numerical models 2o-ZCT-P1 and 2o-ZCT-P2 in the subfigure 5(b) corresponding to the point P_2.

From the numerical results one can observe a good agreement between the solutions given by the three different approaches, namely, the BEV model by Liu and Woo, the second-order BEP model by Zhao et al. and the models developed in this work. We can also conclude that our proposed fourth-order model has better stability properties than the referred second-order models.

7.2 Object moving in an horizontal floor

We simulate a wave generated by an object moving on an horizontal bottom with a constant speed. We consider a two-dimensional simplified version of the moving slide used in the works of Lynett and Liu, 2002 [25] as well as Fuhrman and Madsen, 2009 [26]. The numerical domain is a 30 m line discretized with 300 P_2 elements.

The bottom is defined by $h(x,t) = h_0 + h_1(x,t)$, with $h_0 = 0.45$ m and

$$h_1(x,t) = -\frac{\Delta h}{(1+\tanh(1))^2}\bar{X}(x,t) \tag{48}$$

where

$$\bar{X}(x,t) = \{1+\tanh[2x-2x_l(t)]\}\{1-\tanh[2x-2x_r(t)]\}, \tag{49}$$

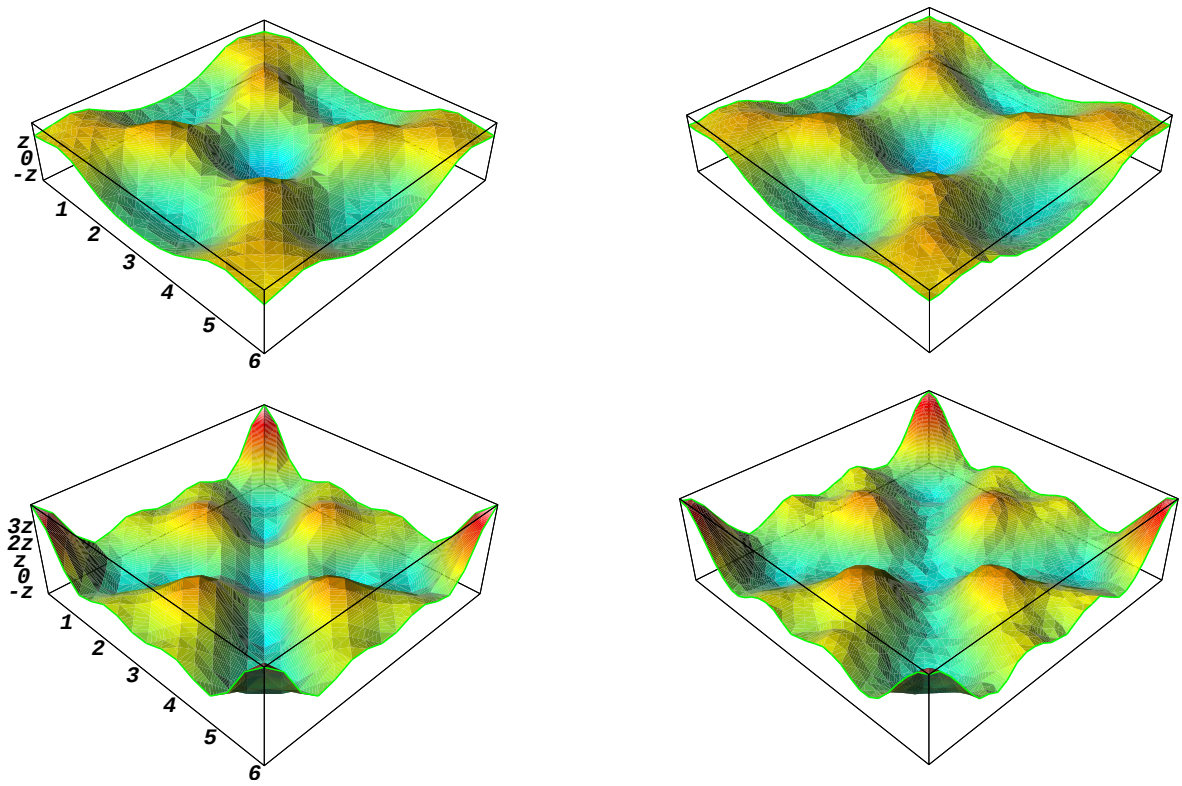

Figure 4: Surface elevation at the time $t_1 = 4$ s and $t_2 = 8$ s. 4o-M-CDG-P2 with a symmetric mesh, $\tau = 0.1$ and $\Delta t = 0.0005$ s (left column). 4o-W-CDG-P2 with an unstructured mesh, $\tau = 0.004$ and $\Delta t = 0.00025$ s (right column). Vertical scale z=0.005 m.

$$x_l(t) = x_c(t) - \frac{1}{2}, \quad x_r(t) = x_c(t) + \frac{1}{2}, \quad x_c(t) = x_0 + S_0 t, \tag{50}$$

with a constant speed $S_0 = 1$ m s^{-1}, $x_0 = 0$ m and $\Delta h = 0.045$ m stands for the maximum thickness of the slide.

We only compare the solutions of the weakly non linear models, namely, 4o-W-CDG-P2 and 2o-ZCT-P2. Note that the later model only incorporates lower order terms for the source function. In Fig. 6 one can observe the evolution of the surface wave generated by the movement of the slide (red) during ten seconds. Full reflective boundaries and zero initial conditions are considered. The main difference of the two tested models lies in the shorter waves in the wake of the wave. Again the 2o-ZCT-P2 model blows-up around $t \approx 8$ s. We can clearly observe that the generated front wave travels at a higher speed than the bottom slide.

8 CONCLUSIONS

A class of sixth and fourth-order Boussinesq type equations is developed for modelling surface water waves. Dissipative effects and wave generation due to moving bottom are

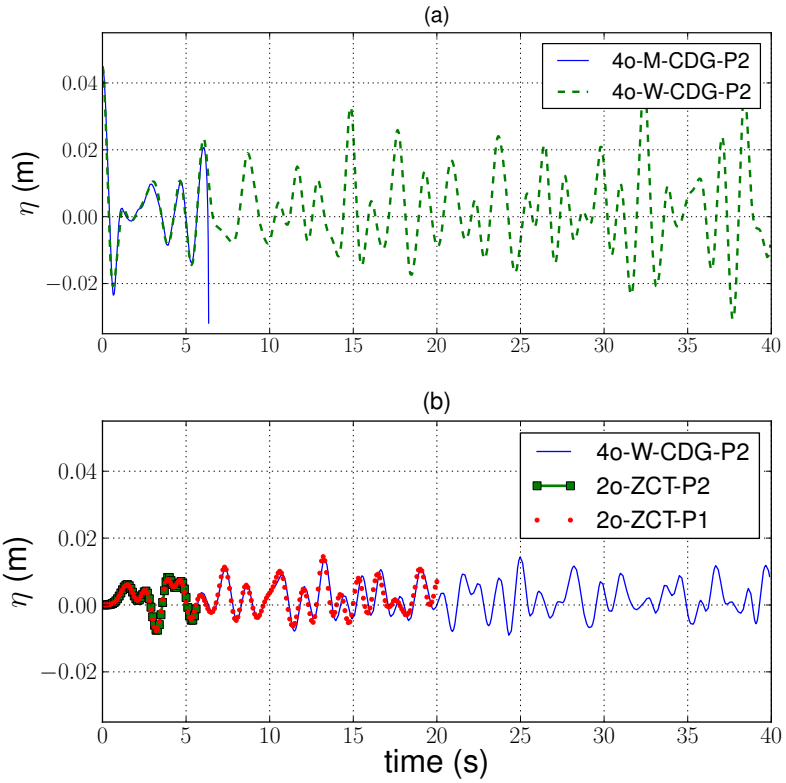

Figure 5: Time history of the surface elevation at $P_1 = (3, 3)$ m (a) and $P_2 = (1, 1)$ m (b) using an unstructured mesh and $\tau = 0.01$. In (a) 4o-M-CDG-P2 and 4o-W-CDG-P2. In (b) 4o-W-CDG-P2, 2o-ZCT-P1 and 2o-ZCT-P2.

considered. Improved dispersion relation characteristics are obtained due to the inclusion of the higher order extra $O(h_0\mu^6)$ term in the velocity potential expansion.

A C/DG-FEM scheme is proposed for the solution of the fourth-order Boussinesq system. Several numerical tests are presented, showing good agreement with the solutions provided by the other models and validating the C/DG numerical method. A drawback of the proposed method is the choice of the penalty parameters. Relations between penalty parameters, mesh size and geometry as well as the time steps should be further investigated. Thus, the convergence of the numerical scheme should be studied in the near future. Note that in the time dependent moving bottom cases, the numerical method may become very time-expensive. This is due to the complexity of the source functions, the need to rebuild the system matrices and vectors at each time step together with the calculation of the element boundary penalty terms. However, this C/DG-FEM scheme has a higher stability than the other ones used in this work.

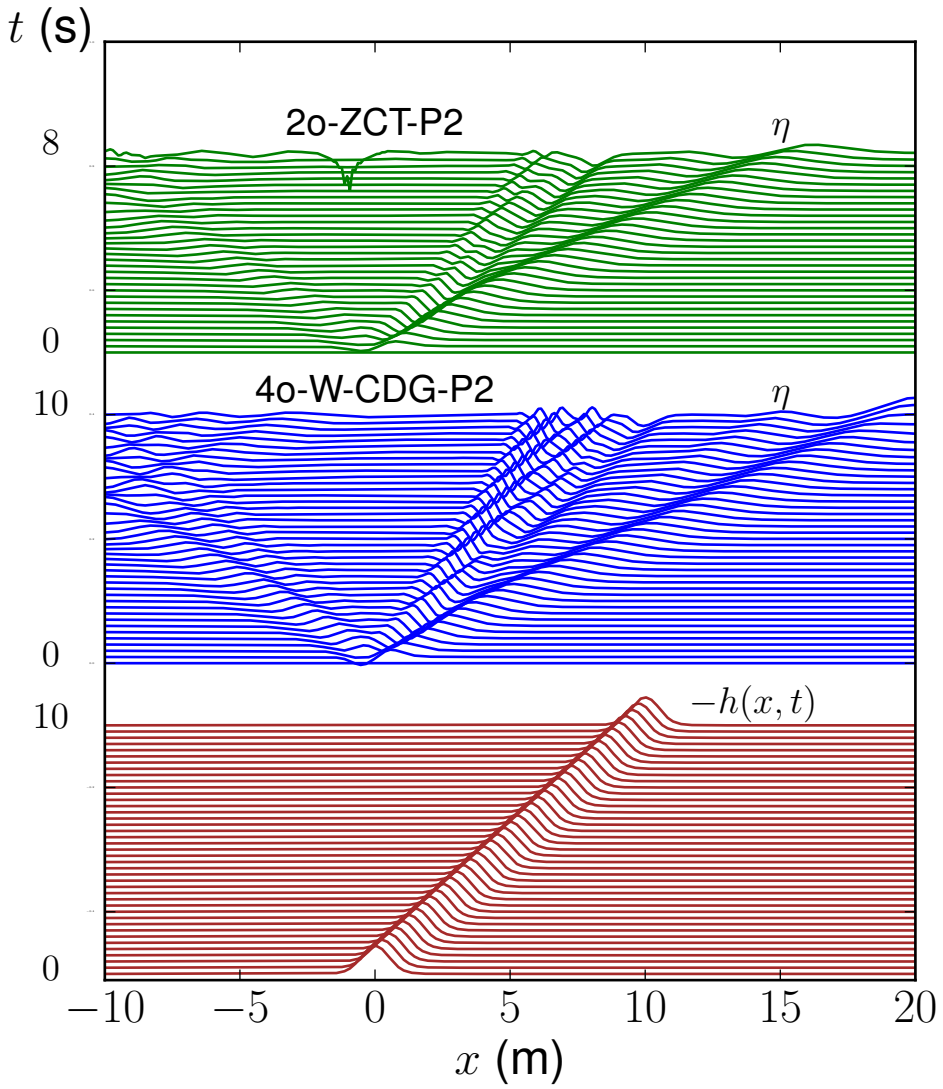

Figure 6: Evolution of the surface wave elevation η and slide positions (red), given by 4o-W-CDG-P2 (blue) and 2o-ZCT-P2 (green). The time step used is $\Delta t = 0.00025$ s and the penalty parameter for 4o-W-CDG-P2 is $\tau = 0.1$.

Acknowledgments

L. Trabucho's work is partially supported by Fundação para a Ciência e Tecnologia, Financiamento Base 2008-ISFL-1-209. N. Lopes' work is supported by Instituto Superior de Engenharia de Lisboa – ISEL.

REFERENCES

[1] Liu P. L.-F. and Woo, S.-B., Finite element model for modified Boussinesq equations i: Model development. *Journal of Waterway, Port, Coastal and Ocean Engineering*, **130**(1):17–28 (2004).

[2] Walkley M. and Berzins M., A finite element method for the two-dimensional extended Boussinesq equations. *Internat. J. Numer. Methods Fluids*, **39**(10):865–885 (2002).

[3] Chen Y. and Liu P. L.-F., Modified Boussinesq equations and associated parabolic models for water wave propagation. *J. Fluid Mech.*, **288**:351–381 (1994).

[4] Zhao M., Teng B. and Cheng L., A new form of generalized Boussinesq equations for varying water depth. *Ocean Engineering* 11, **31**:2047–2072 (2004).

[5] Engel G., Garikipati K., Hughes T. J. R., Larson M. G., Mazzei L. and Taylor R. L., Continuous/discontinuous finite element approximations of fourth-order elliptic problems in structural and continuum mechanics with applications to thin beams and plates, and strain gradient elasticity. *Comput. Methods Appl. Mech. Engrg.*, **191**(34):3669–3750 (2002).

[6] The FEniCS Project. *http://www.fenics.org*.

[7] Olgaard K. B., Logg A. and Wells G. N., Automated code generation for discontinuous Galerkin methods. *SIAM J. Sci. Comput.*, **31**(2):849–864 (2009).

[8] Eskilsson C. and Sherwin S. J., Spectral/hp discontinuous galerkin methods for modelling 2d boussinesq equations. *Journal of Computational Physics*, **212**(2):566 – 589 (2006).

[9] Engsig-Karup A. P., Hesthaven J. S., Bingham H. B. and Warburton T., Dg-fem solution for nonlinear wave-structure interaction using boussinesq-type equations. *Coastal Engineering*, **55**(3):197 – 208 (2008).

[10] Avilez-Valente P. and Seabra-Santos F. J., A high-order Petrov-Galerkin finite element method for the classical boussinesq wave model. *International Journal for Numerical Methods in Fluids*, **59**(9):969–1010 (2009).

[11] Codina R. and González-Ondina J. M., Diaz-Hernández G, Principe J., Finite element approximation of the modified Boussinesq equations using a stabilized formulation. *Internat. J. Numer. Methods Fluids*, **57**(9):1249–1268 (2008).

[12] Dolfwave. *http://www.fenics.org/wiki/DOLFWAVE*.

[13] Dutykh D. and Dias F. Dissipative boussinesq equations. *Comptes Rendus Mecanique*, **335**:559 (2007).

[14] Dias F., Dyachenko A. and Zakharov V., Theory of weakly damped free-surface flows: A new formulation based on potential flow solutions. *Physics Letters A*, **372**(8):1297 – 1302 (2008).

[15] Whitham G. B., *Linear and nonlinear waves*. Wiley-Interscience [John Wiley & Sons]: New York. Pure and Applied Mathematics (1974).

[16] Johnson R., *A Modern Introduction to the Mathematical Theory of Water Waves*. Cambridge Texts in Applied Mathematics, Cambridge University Press, (1997).

[17] Lopes N. D., Pereira, P. J. S. and Trabucho L.,Improved Boussinesq Equations for Surface Water Waves, *Automated Scientific Computing, The FEniCS book*, Springer, submitted.

[18] Dutykh D. and Dias F,. Water waves generated by a moving bottom. *Tsunami and nonlinear waves*. Springer: Berlin, 65–95 (2007).

[19] Nwogu O., Alternative form of boussinesq equations for nearshore wave propagation. *Journal of Waterway, Port, Coastal, and Ocean Engineering*, **119**(6):618–638 (1993).

[20] Gobbi M. F., Kirby J. T. and Wei G., A fully nonlinear Boussinesq model for surface waves. II. Extension to $O(kh)^4$. *J. Fluid Mech.*, **405**:181–210 (2000).

[21] Madsen P.A. and Sorensen O.R., A new form of the boussinesq equations with improved linear dispersion characteristics. part 2. a slowly-varying bathymetry. *Coastal Engineering*, **18**(3-4):183 – 204 (1992).

[22] Madsen P. A. and Schäffer H. A., Higher-order Boussinesq-type equations for surface gravity waves: derivation and analysis. *R. Soc. Lond. Philos. Trans. Ser. A Math. Phys. Eng. Sci.*, **356**(1749):3123–3184 (1998).

[23] Brenner S. C. and Scott L. R., *The mathematical theory of finite element methods*, *Texts in Applied Mathematics*, vol. 15. Third edn., Springer: New York (2008).

[24] Beji S. and Nadaoka K., A formal derivation and numerical modelling of the improved equations for varying depth. *Ocean Engineering*, **23**(8):691–704 (1996).

[25] Lynett P. and Liu P. L.-F., A numerical study of submarine-landslide generated waves and run-up. *Proceedings of the Royal Society of London. Series A: Mathematical, Physical and Engineering Sciences*, **458**(2028):2885–2910 (2002).

[26] Fuhrman D. R. and Madsen P. A., Tsunami generation, propagation, and run-up with a high-order boussinesq model. *Coastal Engineering*, **56**(7):747 – 758 (2009).